Radiation Measurements 153 (2022) 106730

Contents lists available at ScienceDirect

Radiation Measurements

journal homepage: www.elsevier.com/locate/radmeas

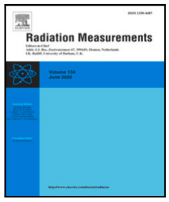

Standardizing the computerized analysis and modeling of luminescence phenomena: New open-access codes in R and Python

Vasilis Pagonis [a,*], George Kitis [b]

[a] McDaniel College, Physics Department, Westminster, MD 21157, USA
[b] Aristotle University of Thessaloniki, Physics Department, Nuclear Physics and Elementary Particles Physics Section, 54124 Thessaloniki, Greece

ARTICLE INFO

Keywords:
Luminescence Dosimetry
R scripts
Computerized Deconvolution of luminescence signals
Python scripts
Open access codes

ABSTRACT

In this paper we describe a new initiative for the development of open-access codes in R and Python, to be used for computerized analysis and modeling of luminescence phenomena. The purpose of this broad initiative is to help in the classification, organization and standardization of the computerized analysis and modeling of a wide range of luminescence phenomena. Although a very significant number of such open access codes is already available in the literature, there is a lack of common standardization and homogeneity in the nomenclature and in the codes, which we hope to address. New open-access codes are developed for thermoluminescence (TL), isothermal luminescence (ITL), optically stimulated luminescence (OSL), infrared stimulated luminescence (IRSL), dose response (DR) and time-resolved (TR) signals. In each of these categories, computer codes are currently being developed based on (a) delocalized transitions involving the conduction/valence bands and (b) localized transitions based on proximal interactions between traps and centers. Whenever applicable, additional codes are developed for semi-localized transition models, which are based on a combination of localized and delocalized transitions. While many previously published codes are based on the empirical general order kinetics and on first order kinetics, several of the new codes in R and Python are based on physically meaningful kinetics described by the Lambert W function. During the past decade, the Lambert W function has been shown to describe both thermally and optically stimulated phenomena, as well as the nonlinear dose response of TL/OSL/ESR in dosimetric materials. The paper demonstrates the proposed classification and organization of the codes, which it is hoped will be a useful tool, especially for newcomers to the field of luminescence dosimetry.

1. Introduction

Phenomenological luminescence models and the associated subject of computerized curve fitting analysis and modeling are an essential part of analysis of thermally and optically stimulated luminescence signals (see for example, the recent review paper by Kitis et al. 2019). Computerized deconvolution of complex luminescence curves into their individual components by using curve fitting methods is widely applied for dosimetric purposes, as well as for evaluating the physical parameters describing the luminescence processes. Although a very significant number of open access codes are already available in the literature, there is a lack of common standardization and homogeneity in nomenclature and in the presentation of the computer codes (see for example Peng et al., 2021; Chung et al., 2011, 2012, 2013; Puchalska and Bilski, 2006; Pagonis et al., 2001; Afouxenidis et al., 2012).

In this paper we describe a new initiative for the development of open-access codes in R and Python, to be used for computerized analysis and modeling of luminescence phenomena. The purpose of this broad initiative is to help in the classification, organization and standardization of the computerized analysis and modeling of a wide range of luminescence phenomena. The new open-access codes are grouped in the broad categories of thermoluminescence (TL), isothermal luminescence (ITL), optically stimulated luminescence (OSL), infrared stimulated luminescence (IRSL), dose response (DR) and time-resolved (TR) codes. Within each of these broad categories, codes are being developed based on (a) delocalized transitions involving the conduction/valence bands and (b) localized transitions based on proximal interactions between traps and centers. Whenever applicable, additional codes are developed for semi-localized transition models, which are based on a combination of localized and delocalized transitions. While most previously published codes for thermally and optically stimulated phenomena are based on the empirical general order kinetics (GOK) and/or on first order kinetics (FOK), the new codes in R

* Corresponding author.
E-mail address: vpagonis@mcdaniel.edu (V. Pagonis).

https://doi.org/10.1016/j.radmeas.2022.106730
Received 4 November 2021; Received in revised form 7 February 2022; Accepted 18 February 2022
Available online 28 February 2022

and Python are also based on physically meaningful kinetics described by the Lambert W function (for a more complete discussion of the importance and use of the Lambert W function in the description of luminescence phenomena, see Section 4.10 in Pagonis, 2021).

The paper is organized as follows: Section 2 presents a general discussion and overview of luminescence models and computerized curve deconvolution analysis (CCDA). This is followed in Section 3 by a summary of the analytical equations for CCDA, and in Section 4 by a general discussion of the computerized curve deconvolution procedures in R and Python. Sections 5 and 6 discuss the open access codes for R and Python respectively. The paper concludes with a general discussion of the current status of this open access codes initiative.

2. Overview of phenomenological luminescence models

Phenomenological luminescence models can generally be classified into two broad general categories, and they were summarized in the recent review paper by Kitis et al. (2019). The first category contains models based on *delocalized* electronic transitions, involving transitions taking place via the delocalized conduction and valence bands. This first category includes several commonly used models for fitting luminescence signals: the first order kinetics model (FOK), General One trap model (GOT), Mixed Order kinetics (MOK) model, and the empirical General Order Kinetics (GOK) model. These delocalized transition models are used routinely for popular dosimetric materials like BeO, LiF: Mg, Ti, Al_2O_3:C, quartz, doped LiB_4O_7 etc.

Models in the second category will be referred to as *localized* models in the rest of this paper. There are several types of such models (for a review of such models and code examples, the reader is referred to Chapters 6–7 in Pagonis, 2021). In this paper we focus on the EST model of Jain et al. 2012, which is based on quantum tunneling processes taking place from the excited state of the trap, within random distributions of electrons and positive charges. In the EST model, the probability of the recombination process taking place depends on the distance between the negative and positive charges in the material. These types of models have been used for analyzing the luminescence signals from many types of feldspars and apatites (Sfampa et al., 2015), as well as for doped YPO4 (Mandowski and Bos, 2011), doped MgB_4O_7 (Pagonis et al., 2019) and other materials.

2.1. Models for analysis of TL and ITL signals

There are four major categories of *delocalized* models found in the luminescence literature, namely first order kinetics (FOK) models, general one trap models (GOT), mixed kinetics order models (MOK) and the empirical general order kinetics models (GOK). These models lead to analytical equations which are commonly used for the analysis of TL signals, and which are summarized in Fig. 1. The last entry in Fig. 1 is the excited state tunneling model (EST), which is a *localized* transitions model (Jain et al. 2012).

The specific nomenclature used for the analytical equations in Fig. 1 and in the rest of this paper, is our effort to classify and standardize the names used for these equations in the literature. The acronyms KV and KP in this figure refer to the Kitis–Vlachos and Kitis–Pagonis equations respectively, and are explained in Section 3 of this paper.

Several of the equations listed in Fig. 1 are available in two mathematical versions, the original and the transformed versions (see the detailed discussion in Kitis et al. 2019). The two mathematical versions of these equations are discussed in Section 3.

Due to the space limitation for this conference paper, it is not possible to list al equations in this initiative. Instead, we refer the reader to the review paper by Kitis et al. (2019) and to the recent book by Pagonis (2021).

ITL signals can also be described within the FOK, GOT, MOK, GOK and EST models, similar to the situation for TL signals. These five models lead to analytical equations which are commonly used for the analysis of ITL signals, and they are summarized in Fig. 2.

2.2. Models for analysis of OSL signals

When the stimulation of a sample is optical using visible light, one is dealing with *optically stimulated luminescence* (OSL). Typically, blue LEDs with a wavelength of 470 nm are used during these OSL experiments. When the stimulation is with visible light and also occurs with a source of constant light intensity, the stimulated luminescence is termed *continuous wave optically stimulated luminescence* (CW-OSL). However, when the optical stimulation takes place using a source with an intensity which increases linearly with time, the stimulated luminescence is called *linearly modulated optically OSL* (LM-OSL).

OSL signals can also be described by the FOK, GOT, MOK, GOK and EST models, similar to the situation for TL signals. These five models lead to analytical equations which are commonly used for the analysis of OSL signals, and they are summarized in Fig. 3.

2.3. Models for analysis of IRSL signals

When the optical stimulation of the irradiated sample takes place with infrared photons, this process is called *infrared stimulated luminescence (IRSL)*. Typically infrared LEDs with a wavelength of 850 nm are used during these IRSL experiments. During CW-IRSL experiments the intensity of the light is kept constant, resulting in most cases in a monotonically decaying curve. Linear modulation of the infrared LEDs results in the production of a peak shaped LM-IRSL signal.

The shapes of CW-OSL and LM-OSL signals are very similar to the shapes of CW-IRSL and LM-IRSL signals. However, these signals are obtained with very different wavelengths of light (470 nm for blue light LEDs and 850 nm for infrared LEDs). Extensive research has shown that the mechanisms involved in the production of these signals are very different. In the case of the CW-OSL and LM-OSL signals from most dosimetric materials, the mechanism is believed to involve the conduction band due to the higher energy of the blue LEDs, and can be described by a *delocalized* model.

In the case of the CW-IRSL and LM-IRSL signals, the production mechanism is believed to involve localized energy levels located between the conduction and valence bands. There are several versions of this type of a *localized transition model* in the literature; in this paper we limit our discussion to the excited state transition (EST) models, which have been used extensively to describe quantum tunneling luminescence phenomena in feldspars (Sfampa et al., 2015), apatites (Polymeris et al., 2018), doped YPO4 (Mandowski and Bos, 2011), and doped MgB_4O_7 (Pagonis et al., 2019).

The EST model leads to analytical equations which are commonly used for the analysis of CW-IRSL and LM-IRSL signals, and they are summarized in Fig. 4.

2.4. Models for analysis of dose response

Fig. 5 is a schematic showing several types of models which have been used for describing the dose response of luminescence signals. Of these models, the OTOR model and two trap one recombination center (TTOR) model are based on systems of differential equations, and lead to the saturating exponential (SE) function and the Pagonis–Kitis–Chen equations (PKC and PKC-S) which are discussed in Section 3. The GOK, double saturating exponential (DSE) and SE plus linear (SEL) equations shown in Fig. 5 can be considered empirical, since they do not arise directly from a mathematical model based on electronic transitions taking place in a solid.

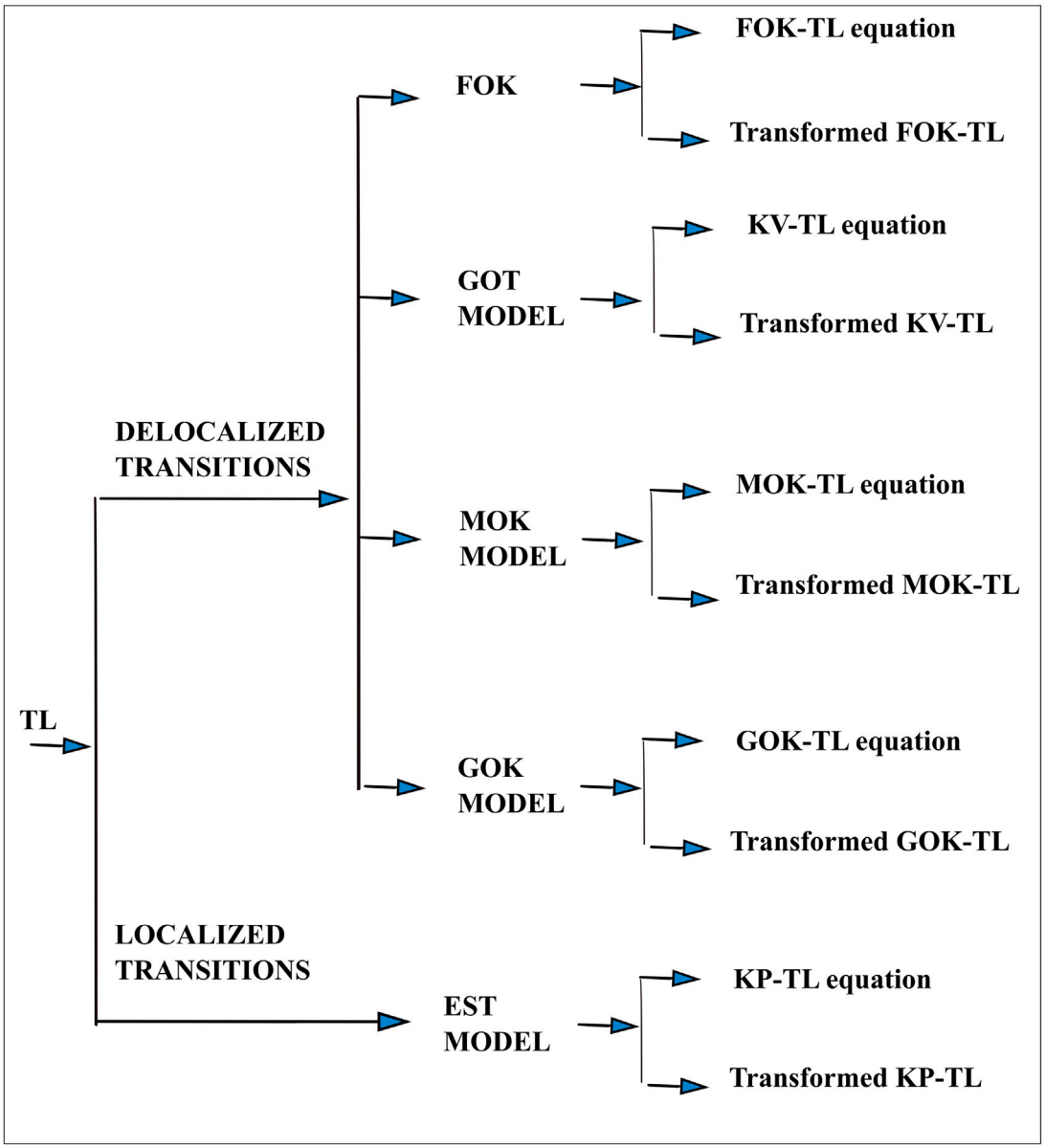

Fig. 1. Schematic diagram of the main models used for analyzing TL signals and the respective analytical equations. Four of these models are based on *delocalized* transition models: the first order kinetics (FOK), general one trap (GOT), mixed order kinetics (MOK) and general order kinetics (GOK) empirical model. The excited state tunneling model (EST) is a *localized transitions* model.

2.5. Models for analysis of time resolved (TR) signals

TR experiments can provide crucial information about the luminescence mechanisms in a dosimetric material. Fig. 6 is a schematic showing several types of models which have been used for describing the dose response of luminescence signals.

Delocalized transition models which have been used in order to describe TR-OSL experimental data obtained with blue LEDs (see the review paper by Chithambo et al. 2016, and references therein). The most popular delocalized transition model has been the FOK-TR model, in which the excitation period of the TR experiment is described by the sum of saturating exponential function, and the relaxation stage of the TR experiment is described by the sum of decaying exponential functions. The FOK-TR model has been used extensively, for example, for TR-OSL measurements in quartz. In addition, stretched exponential functions have been suggested as a possible fitting function to described the relaxation stage of TR experiments (see for example Pagonis et al. 2012).

Localized transition models have been used to describe TR-IRSL experimental data obtained with infrared LEDs (Chithambo et al. 2016, Pagonis et al. 2012).

3. Analytical equations and their transformed equivalents

A useful technique for developing new analytical equations for computerized analysis of data, is to develop *transformed* analytical equations which use parameters that can be estimated directly from the experimental data. The general method of developing the transformed versions of the analytical equations is described in detail in the review paper by Kitis et al. (2019). The transformation is based on replacing two of the variables in the equations with two new variables. For example in the case of TL signals, the initial concentration of trapped electrons n_0 and the frequency factor s in the equations, will be replaced with the maximum intensity I_m and the corresponding temperature T_m.

For a recent extensive compilation of the literature on the computerized glow curve deconvolution (CGCD) software used and developed for

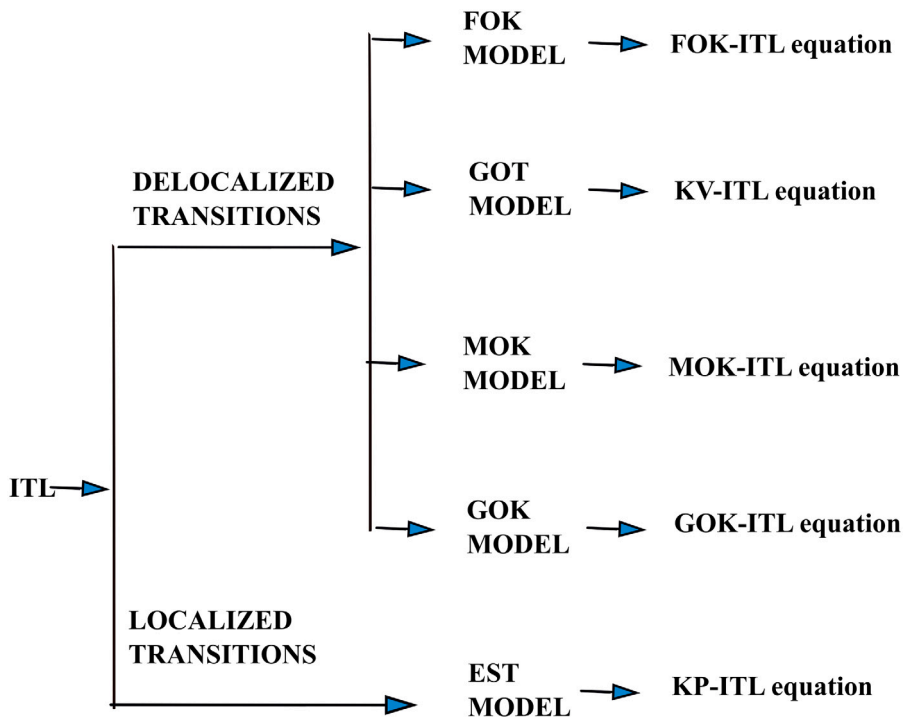

Fig. 2. Schematic diagram of the main delocalized and localized models which are used in this literature for analysis of ITL signals, and the respective analytical equations.

radiation dosimetry, the reader is referred to the paper by Peng et al. (2021). These authors also presented a unified presentation of CGCD within the framework of the open source R package `tgcd` Peng et al. 2016, and included first, second, general, and mixed-order kinetics models for delocalized transitions.

Kitis et al. (1998) developed transformed equations for first, second and general order kinetics under a linear heating function. In later works transformed equations were developed by Kitis and Gómez-Ros (1999) and Gómez-Ros and Kitis (2002) for mixed order kinetics and for continuous trap distributions, and by Kitis et al. (2012) for an exponential heating function. In the area of OSL, Kitis and Pagonis (2008) developed transformed equations for LM-OSL signals. Recently Sadek et al. (2015) transformed the analytical expression derived from the OTOR model, whereas Kitis and Pagonis (2014) developed transformed analytical expressions for tunneling recombination from the excited state of a trap.

3.1. The Kitis–Vlachos (KV) equations for TL, ITL, CW-OSL and LM-OSL signals

Kitis and Vlachos (2013) were able to solve analytically the GOT model. Later Singh and Gartia (2013) obtained the analytical solution using the omega function. Kitis and Vlachos (2013) obtained the following general analytical expression for the intensity $I(t)$ of the luminescence signal, when $R < 1$:

$$I(t) = \frac{N\,R}{(1-R)^2}\,\frac{p(t)}{W[e^z] + W[e^z]^2} \tag{1}$$

$$z(t) = \frac{1}{c} - \ln(c) + \frac{1}{1-R}\int_0^t p(t)\,dt \tag{2}$$

$$c = \frac{n_0}{N}\,\frac{1-R}{R} \tag{3}$$

where n_0 and N are the initial and total concentrations of filled traps, $R = A_n/A_m$ is the dimensionless retrapping ratio of the retrapping and recombination coefficients in the OTOR model, and $p(t)$ is the excitation rate for the experimental mode. $W[e^z]$ is the Lambert W function (Corless et al. 1996; Corless et al. 1997). This function is the solution $y = W[e^z]$ of the transcendental equation $y + \ln y = z$. In these analytical equations W represents the *real positive part* of the Lambert W function. In fact, Kitis and Vlachos (2013) found that there is a second solution of the OTOR model corresponding to $R > 1$. However, for our deconvolution purposes, we need only concern ourselves with the positive real branch of W, since values of the retrapping ratio R in the range $0 < R < 1$ can describe any luminescence signal between first and second order kinetics. Kitis et al. (2019) termed this general equation the *first master equation*, and in this paper we refer to it as the *Kitis–Vlachos equation (KV equation)* for thermally/optically stimulated phenomena. The term *master equation* was introduced because the equation is very general and can describe a wide variety of luminescence signals originating in *delocalized* electronic transitions (TL, ITL, CW-OSL, LM-OSL), by simply using a different mathematical expression for the excitation rate $p(t)$. For thermally stimulated phenomena, the trap is characterized by the thermal activation energy E (eV) and by the frequency factor s (s^{-1}). Respectively for optically stimulated phenomena, the trap is characterized by the optical cross section σ of the OSL or IRSL process.

Table 1
Table of the KV-equations for analysis of TL, ITL, CW-OSL and LM-OSL signals. The equations in this table refer to the *delocalized* GOT model of TL described in this chapter.

Type of signal	Equation	Stimulation rate $p(t)$ (s^{-1})	Model parameters
TL	**KV-TL**	$s\,\exp\{-E/(kT)\}$	$R,\ N,\ n_0$
ITL	**KV-ITL**	$s\,\exp\{-E/(kT_{ISO})\}$	$R,\ N,\ n_0$
CW-OSL	**KV-CW**	$\sigma\,I = \lambda$	$R,\ N,\ n_0$
LM-OSL	**KV-LM**	$\sigma\,It/P = \lambda t/P$	$R,\ N,\ n_0$

The various forms of the KV equation are summarized in Table 1. The nomenclature used here is rather obvious, with KV-ITL referring to the Kitis–Vlachos equation for ITL signals etc.

3.2. The Kitis–Pagonis (KP) equations for TL, ITL, CW-IRSL and LM-IRSL signals

Kitis and Pagonis (2013) derived an analytical equation solution for the EST model, by considering quasi-equilibrium conditions (QE).

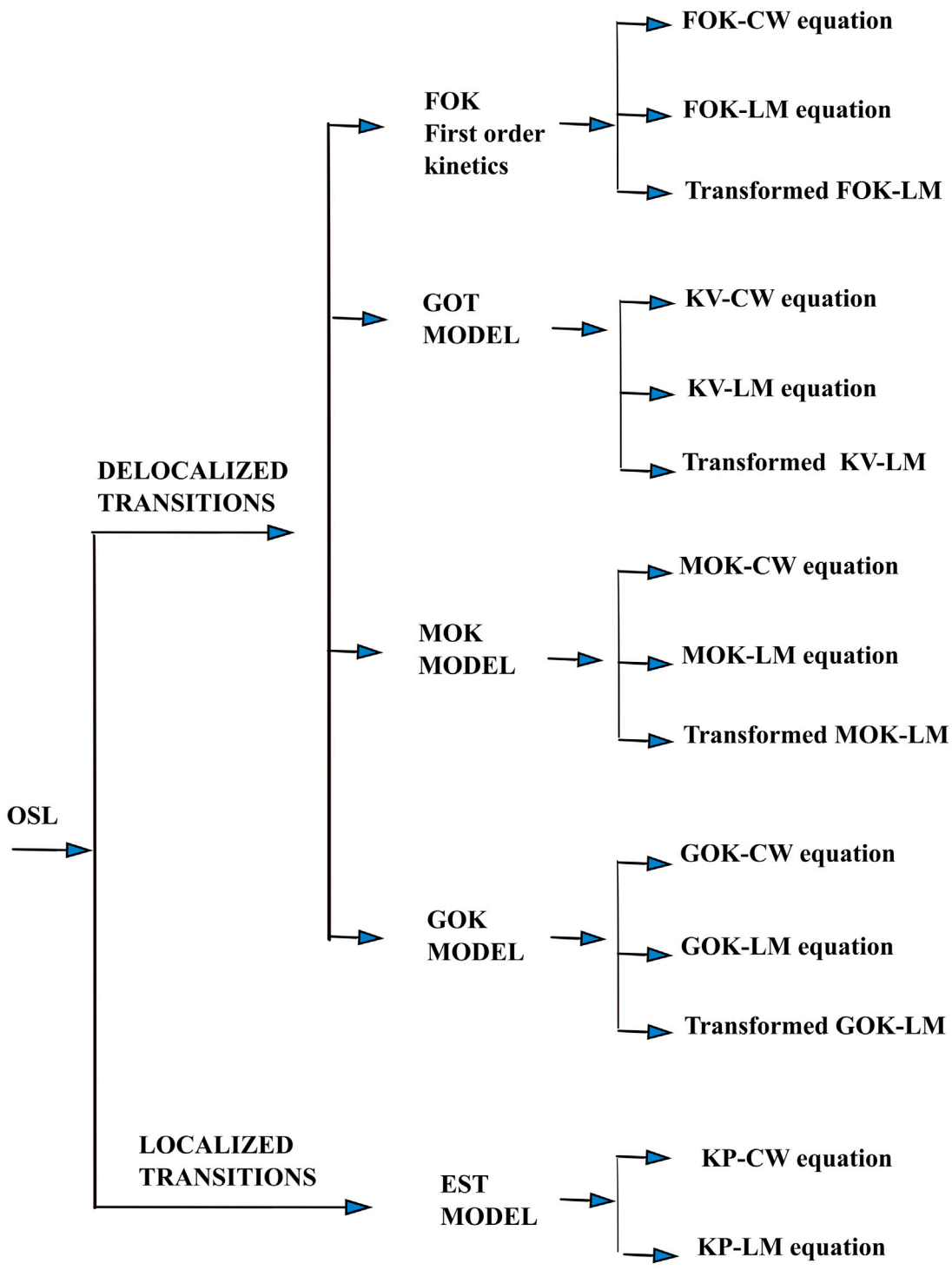

Fig. 3. The main models which are used for analysis of CW-OSL and LM-OSL signals, and the respective analytical equations.

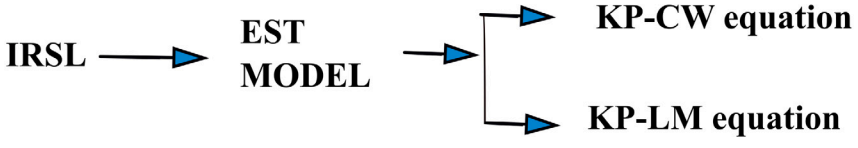

Fig. 4. Schematic diagram showing the analytical equations from the *localized* model EST, which are used for analysis of CW-IRSL and LM-IRSL signals.

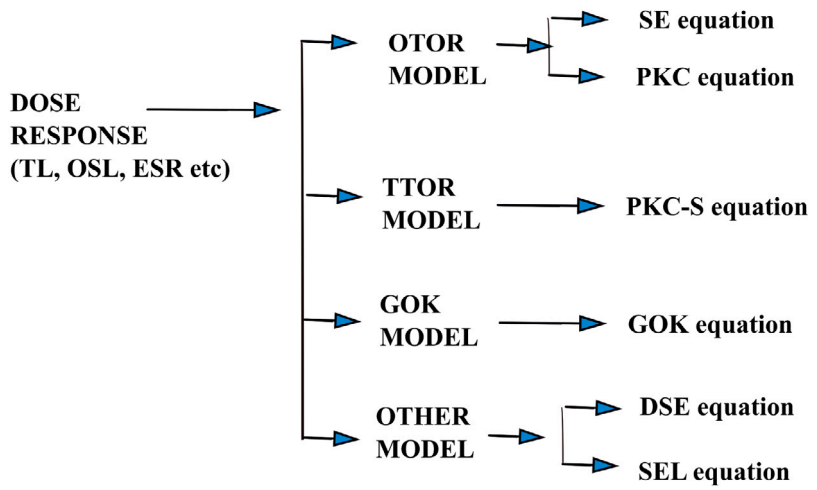

Fig. 5. Schematic diagram showing the two *delocalized* models OTOR and TTOR models discussed in this paper, and the respective analytical equations which are used for analysis of the dose response of luminescence signals.

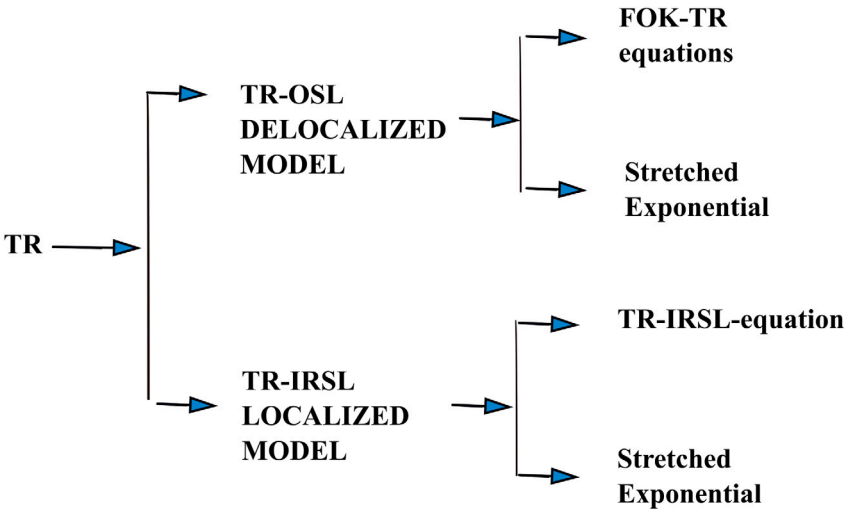

Fig. 6. Schematic diagram showing several models and the respective analytical equations which are used for analysis of the time-resolved luminescence signals.

These authors carried out extensive algebra, and obtained the following analytical solutions for the luminescence intensity $I(t)$ during thermally or optically stimulated luminescence experiments. We will refer to this analytical equation as the *general Kitis–Pagonis equation (KP equation)*:

$$I(t) = 3\, n_0\, \rho'\, 1.8\, A(t)\, F(t)^2\, e^{-F(t)}\, e^{-\rho' (F(t))^3} \tag{4}$$

$$F(t) = \ln\left(1 + \frac{1.8\, s_{tun}}{B'} \int_0^t A(t)\, dt\right) \tag{5}$$

where $A(t)$ (s^{-1}) is the excitation rate from the ground state into the excited state of the trap, ρ' is dimensionless acceptor density, B' (s^{-1}) is the retrapping rate from the excited state into the ground state of the trap, and s_{tun} (s^{-1}) is the frequency factor for the tunneling process.

Eq. (4) was termed the *fifth master equation* in the review paper by Kitis et al. (2019). This is because it is very general and like the KV-equations, it can also describe a wide variety of luminescence signals originating in *localized* electronic transitions (TL, ITL, CW-IRSL, LM-IRSL), by simply using a different mathematical expression for the excitation rate $A(t)$. The KP equations can characterize TL, IRSL and ITL signals within the EST model, as long as one is dealing with freshly irradiated samples, i.e. samples which have not undergone any thermal or optical treatments after irradiation. The reason is that these types of treatments cause a truncation in the distribution of nearest neighbors in the crystal. For a detailed discussion of this topic, see Section 6 in Pagonis et al. (2021).

The fifth master equation Eq. (4) was tested by Kitis and Pagonis (2013), by comparing it with the numerical solution of the differential equations in the EST model (Kitis and Pagonis 2013; Kitis and Pagonis 2014; Pagonis and Kitis 2015). This equation has been also tested extensively during the past decade, by comparing it with many different types of experimental signals, from different types of natural and artificial dosimetric materials (Sfampa et al. 2014; Şahiner et al. 2017; Kitis et al. 2016; Polymeris et al. 2017).

Detailed examples of using these analytical equations to fit experimental data are given in the recent comprehensive feldspar study by Pagonis et al. 2021 and in the book by Pagonis (2021).

Table 2 summarizes the KP equations which describe TL, ITL, CW-IRSL and LM-IRSL signals within the EST model.

3.3. The Pagonis–Kitis–Chen (PKC and PKC-S) equations for dose response of luminescence signals (TL, OSL, ESR etc.)

The GOT model for irradiation processes leads to the *Pagonis–Kitis–Chen (PKC) equations* for dose response of luminescence signals. Specifically, Pagonis et al. (2020a) developed recently the *exact* analytical solution $n(D)$ of the GOT equation in terms of the Lambert W

Table 2
Table of the KP-equations for analysis of TL, ITL, CW-IRSL and LM-IRSL signals. The equations in this table refer to the *localized* EST model of luminescence developed by Jain et al. (2012).

Type of signal	Equation	Stimulation rate $A(t)$ (s^{-1})	Model parameters
TL	**KP-TL**	$s\ \exp\{-E/(kT)\}$	$n_0,\ \rho',\ s,\ E$
ITL	**KP-ITL**	$s\ \exp\left\{-E/\left(kT_{ISO}\right)\right\}$	$n_0,\ \rho',\ s,\ E$
CW-IRSL	**KP-CW**	$\sigma\ I = \lambda$	$n_0,\ \rho',\ \lambda$
LM-IRSL	**KP-LM**	$\sigma\ It/P = \lambda t/P$	$n_0,\ \rho',\ \lambda$

function:

$$\frac{n(D)}{N} = 1 + \frac{1}{1-R} W\left[(R-1)\exp\left(R-1-D/D_c\right)\right] \tag{6}$$

where the constant D_c is defined as $D_c = N/R$, R is the retrapping ratio in the OTOR model, and $n(D)/N$ is the trap filling ratio The parameter D_c has the same units as the dose D, and depends on the physical properties R, N of the material. From a physical point of view, the retrapping ratio parameter R can have *any* positive real value, including values $R > 1$. The values $R \to 0$, $R \to 1$ correspond to first and second order kinetics. Furthermore, under certain physical assumptions, values of R between 0 and 1 correspond to the empirical general order intermediate kinetic orders (see for example the discussion in Kitis et al. 2019). As may be expected from a physical point of view, the approach to saturation and the shape of the $n(D)$ function depends on the amount of retrapping, i.e. on the value of the ratio R.

The model of Bowman and Chen (1979) is a TTOR model, which describes superlinear dose response as being a result of competition between two electron traps during the irradiation stage of a sample. Recently Pagonis et al. (2020b) obtained the following Pagonis–Kitis–Chen-Superlinearity (PKC-S) equation, which describes the non-linear dose response of a dosimetric trap:

$$\frac{n(D)}{N} = 1 - \left(\frac{1}{B} W\left[B\exp(B)\exp\left(-D/D_c\right)\right]\right)^{A_2/A_1}. \tag{7}$$

where the two constants B, D_c are functions of the parameters in the original model. The dose response $n(D)/N$ in this rather simple Eq. (7) depends on only three parameters, the constants A_2/A_1, B and D_c. The parameter D_c has the same dimensions at the irradiation dose D, so that the ratio D/D_c in Eq. (7) is dimensionless. The parameter B is also dimensionless and one of the assumptions in this equation is the additional condition $A_2/A_1 < 1$. The overall dose response in this model will depend on the numerical values of the three parameters appearing in these equations: B, D_c, A_2/A_1. As the competitor trap approaches saturation, the dose response of the dosimetric trap n/N becomes superlinear. The initial short linear range in the curve n/N is followed by a range of superlinearity, which eventually becomes sublinear on its way to saturation.

The shape of the simulated dose response $n(D)/N$ from Eq. (6) depends strongly on the retrapping ratio R, and looks similar to a saturating exponential function (SE). The SE is often used to fit experimental dose responses in a variety of materials, and for a variety of luminescence signals, together with two more general equations, the SEL and the DSE functions (Berger and Chen 2011). As noted above, the SEL and DSE are considered more or less empirical analytical equations, and the constants in some of these models are not usually assigned a direct physical meaning. In recent experimental work, the SEL and DSE functions have been used to fit experimental ESR data (Duval 2012; Trompier et al. 2011); OSL data (Lowick et al. 2010; Timar-Gabor et al. 2012; Timar-Gabor et al. 2015; Anechitei-Deacu et al. 2018; Fuchs et al. 2013, Li et al. 2016), TL data (Berger and Chen 2011; Berger 1990; Bosken and Schmidt 2020), and ITL data (Vandenberghe et al. 2009).

For extensive examples of fitting TL,OSL, ESR data using the PKC and PKC-S equations, see the papers by Pagonis et al. 2020a; Pagonis et al. 2020b.

3.4. Analytical equations for the analysis of TR signals

As discussed above, the first order kinetics model is routinely used to describe TR-OSL signals, by using the sum of saturating exponentials and exponential decay functions, which we denote in Fig. 6 as the *FOK-TR equations*.

Pagonis et al. (2016) used the model of Jain et al. (2012) to describe quantitatively the shape of TR-IRSL signals during and following short infrared pulses on feldspars, in the microsecond time scale. These authors developed the following analytical *TR-IRSL equations* for the — light emission, using the assumption of a weak de-excitation rate taking place from the excited state into the ground state of the trap:

$$I_{ON}(t) = I_0\left\{1 - \exp\left(-\rho'\ \ln\left[1.8\ s_{tun}\ t\right]^3\right)\right\} \qquad t < t_0 \tag{8}$$

$$I_{OFF}(t) = I_0\left\{\exp\left(-\rho'\ \ln\left[1.8\ s_{tun}\ t\right]^3\right) - \exp\left(-\rho'\ \ln\left[1.8\ s_{tun}\ (t+t_0)\right]^3\right)\right\} \qquad t > t_0 \tag{9}$$

The parameters in these equations are the saturation intensity I_0, the dimensionless positive charge density ρ', the elapsed time t (s), the tunneling frequency s_{tun} (s^{-1}), the duration of the IR pulse t_0 (s). It is noted that if the assumption of a weak de-excitation rate is lifted in this model, the resulting analytical expressions of $I_{ON}(t)$ and $I_{OFF}(t)$ represent simple exponential functions; this type of exponential behavior has not been reported in TR-IRSL experiments, which are generally believed to follow non-exponential behavior (Pagonis et al., 2016).

In addition to the above TR-IRSL equations, the stretched exponential function has also been used to described the relaxation stage of TR-IRSL experiments (see for example Pagonis et al., 2012).

4. Computerized curve fitting analysis in Python and R

The subject of computerized curve fitting analysis is an essential part of analysis of thermally and optically stimulated luminescence signals, and several sophisticated curve deconvolution techniques have been developed. The general term computerized curve deconvolution analysis (CCDA) is commonly used for any luminescence signal, and in the case of TL signals the term computerized glow curve deconvolution (CGCD) is used extensively. Chen and McKeever (1997) and Chen and Pagonis (2011) summarized the curve fitting procedures commonly used to analyze multi-peak luminescence curves. They emphasized the primary importance of using a carefully measured curve, since any errors in measuring the data can lead to the wrong results in the computerized procedures.

The analysis of complex luminescence signals starts by defining denote the mathematical function $f(T)$ of an individual signal component. When several luminescence components are involved, the glow curve can be written as the linear combination of these analytical functions $f(T)$. Basically, the process of curve fitting, be it for a single or a composite curve, consists of a first guess of the parameters, evaluating $I(T)$ and comparing it to the experimental curve. The parameters are then changed so that the difference between the experimental and calculated curves is minimized. A popular way of doing this is the Levenberg–Marquardt nonlinear least-squares fitting, which minimizes the objective:

$$f = \sum_{i=1}^{n}\left(y_i^{expt} - y_i^{fit}\right)^2, \qquad i = 1 \ldots n \tag{10}$$

where y_i^{expt} and y_i^{fit} are the i-th experimental point and the fitted value respectively, and n is the number of data points. When the weights of the experimental data points are known, one can use the "chi-squared" function instead (Chen and Pagonis, 2011). At the end of the least squares fitting process of minimization of the objective function, one wishes to evaluate the goodness of fit. The goodness of fit of the

equation to the data is often expressed by the Figure of Merit (FOM) which is defined as follows (Balian and Eddy 1977):

$$FOM = \frac{\sum_{i=1}^{n} \mid y_i^{expt} - y_i^{fit} \mid}{\sum_{i=1}^{n} \mid y_i^{fit} \mid}, \qquad i = 1 \ldots n \tag{11}$$

where y_i^{expt} and y_i^{fit} were defined above. Since the FOM is normalized by the integral under the curve, the goodness of fit may be compared from one glow curve to another. Fits are considered to be acceptable when the FOM is of a few percent.

Obviously, one wishes to get a *global minimum* of the objective function, in order to obtain the best possible set of parameters. Unfortunately, non-linear functions of this sort usually have many *local minima*, and practically all the methods of minimization lead to a local minimum which is not necessarily global. A wide variety of methods are being used for such minimization and for increasing the probability of approaching the global minimum, even when the initial guess of the set of parameters is rather far from the final optimum. Some of these methods are steepest descent, Newton, quasi-Newton, simulated annealing and genetic algorithms (Adamiec et al. 2004; Adamiec et al. 2006). In general, it is important to compare the results between different CCDA models, in order to assess the reliability of the determined parameters.

In this paper we use the `optimize()` function in Python to perform CCDA analysis of TL glow curves. Specifically we import and use the function `curve_fit()` in the form:

```
scipy.optimize.curve_fit(f, xdata, ydata, p0, bounds)
```

Here `f` is the function which is used to fit the data (xdata,ydata), `p0` is an array containing the initial guesses for the parameters, and `bounds` specifies the lower and upper bounds on the parameters.

For the R codes discussed in this paper, we use the `nls.LM()` function in the R package `minpack.lm` (see Moré, 1977), available for free download at CRAN (2022). This package implements the Levenberg–Marquardt algorithm, for solving nonlinear least-squares problems which was modified in order to support lower and upper parameter bounds in the fitting parameters. The general structure of the least squares part of the algorithm is

```
nlsLM(formula, data, start, bounds)
```

where `formula` is the analytical equation to be used in the fitting procedure, `data` is the list of experimental data to be fitted, and `start` and `bounds` respectively are the lists of starting and bounding values to be used for the fitting parameters.

When applying CCDA methods of analysis, one should keep in mind that the solutions of the best fit process are not unique, and that therein general are infinite combinations of the parameters which could give a very good fit. Indeed, the results of the CCDA procedures are in many cases strongly influenced by the choice of initial values for the parameters. These are well known standard issues with optimization functions, and they are certainly not unique to luminescence data analysis. It is highly recommended that researchers use several different methods to evaluate the best parameters characterizing a luminescence signal, and not simply use a single fitting method. By using several different methods to analyze the results of different experiments on the same sample, a better understanding and confidence is obtained for the underlying luminescence process.

5. The open access R codes

The past decade has seen rapid growth in the development and application of the programming language R, in the fields of radiation dosimetry, luminescence dosimetry, and luminescence dating. R is now widely used in these scientific areas with new packages becoming available and used regularly by students and researchers (see for example Peng et al. 2021, Peng et al. 2016, Kreutzer et al. 2012, Kreutzer et al. 2017).

Presently, there are 99 fully developed open access R codes available within this initiative. For a detailed description of the various models and R codes, the reader is referred to the recently published book by Pagonis (2021). Fig. 1 shows a schematic diagram of the organization of the 99 R codes in this book. Overall the book is organized in four parts I–IV and 12 chapters, as shown in this diagram.

Part I of the book consists of a practical guide for analyzing luminescence signals having their origin in delocalized transitions, and provide a detailed presentation of various methods of analyzing and modeling experimental data for TL signals, OSL signals, TR-OSL signals and the Dose response of dosimetric signals. *Part II* is a practical guide for analyzing luminescence signals having their origin in localized transitions between energy states located between the conduction and valence bands. It contains a general introduction to quantum tunneling processes, as pertaining to dosimetric materials with emphasis on the analysis of luminescence signals from feldspars and apatites, which exhibit quantum tunneling luminescence phenomena.

Part III provides a general description of luminescence phenomena as a stochastic process, by using Monte Carlo techniques for the description of TL and OSL phenomena. *Part IV* presents several commonly used comprehensive phenomenological models for quartz and feldspars, which are two of the best studied natural luminescence materials. This part also contains simulations of several commonly used experimental protocols for luminescence dating, including the very successful single aliquot regenerative protocol (SAR).

These 99 open access R codes can be downloaded at the GitHub website

https://github.com/vpagonis/Springer-R-book

and a detailed description of the respective equations and models can be found in Pagonis (2021).

6. The open access Python codes

Python is one of the most often used programming languages in the sciences (Van Rossum and Drake 2009). It is a simple and readable language, which makes it relatively easy for developers to find and solve software issues. Two additional big advantages are the existence of an extensive Python community, and compatibility with various platforms. It also supports both procedure-oriented and object-oriented programming, and many libraries exist for carrying out specific scientific tasks.

However, there are currently no open-access scripts available in Python for the deconvolution of TL signals. The advantages of the Python scripts presented in this paper are: they are stand alone codes, user friendly, easy to modify and run for the analysis of single or multiple-peak TL glow curves of most dosimetric materials. The scripts do not require special packages to run, and users can obtain the result of the CCDA analysis in most cases within seconds. The scripts also do not require compilation of code written in FORTRAN or C++, as is the case for some of the other available open-access codes (Peng et al. 2021).

At the present stage in the initiative, there are 24 fully developed open access Python codes. Table 1 shows a listing of the 24 Python codes, consisting of 4 groups: the first group contains 10 Python codes labeled (1.1–1.10) in Table 1, which can be used for deconvolution of TL signals from delocalized transition models. The second group consists of 7 Python codes, with the first five codes labeled (2.1–2.5) being examples of deconvolution of TL signals from *localized* transition models. Codes (3.1–3.3) are an example of applying three different methods of analysis (isothermal signal analysis, initial rise analysis and CGCD analysis), to the popular dosimetric material LiF:Mg,Ti.

The fourth group of Python codes in Table 1 consists of 6 codes labeled (4.1–4.6), providing examples of fitting different types of dose responses (TL, OSL, ESR) to experimental data from various materials.

These 24 Python codes and a detailed description of the respective equations and models can be downloaded at the GitHub website
https://github.com/vpagonis/Python-Codes

The goal of the initiative is to develop a complete set of Python codes for CCDA of luminescence signals, similar to the currently available set of 99 R codes.

Table 3
List of 24 currently available open access Python codes. The last column indicates the corresponding luminescence model: GOT = general one trap model, MOK = mixed order kinetics, FOK = first order kinetics, GOK = general order kinetics, EST = excited state tunneling, GST = ground state tunneling, OTOR = one trap one recombination center, TTOR = two traps one recombination center.

Code	Description of Python code	Model
1.1	Deconvolution of GLOCANIN TL with the KV-TL equation	GOT
1.2	Deconvolution of LiF peak using the KV-TL equation	GOT
1.3	Deconvolution of TL for Al2O3:C using the MOK-TL equation	MOK
1.4	Deconvolution of TL for BeO with transformed MOK-TL	MOK
1.5	Deconvolution of GLOCANIN TL using the original GOK-TL	GOK
1.6	Deconvolution of Al2O3:C glow curve using the GOK-TL	GOK
1.7	Deconvolution LBO data using the transformed KV-TL equation	GOT
1.8	Deconvolution of TL user data (.txt file, GOK-TL)	GOK
1.9	Deconvolution of 9-peak glow curve using the transformed KV-TL	GOT
1.10	Deconvolution of 9-peak GLOCANIN TL data using GOK-TL	GOK
2.1	Anomalous fading (AF) and the g-factor	GST
2.2	Fit MBO data with KP-TL equation	EST
2.3	Fit TL for KST4 feldspar with KP-TL equation	EST
2.4	Deconvolution of 5-peak glow curve for BAL21 sample	EST
2.5	Deconvolution of MBO data with transformed KP-TL equation	EST
3.1	Isothermal analysis for LiF:Mg,Ti	FOK
3.2	Initial rise analysis for LiF:Mg,Ti	
3.3	CGCD analysis of single TL peak in LiF:Mg,Ti	FOK
4.1	Fit dose response of TL data with saturating exponential	Empirical
4.2	Fit of TL dose response data using the PKC equation	OTOR
4.3	Fit of ESR dose response data using the PKC equation	OTOR
4.4	Fit of OSL dose response data using the PKC equation	OTOR
4.5	Fit of TL dose response of anion deficient aluminum oxide (PKC-S)	TTOR
4.6	Fit to Supralinearity index f(D) using the PKC-S equation	TTOR

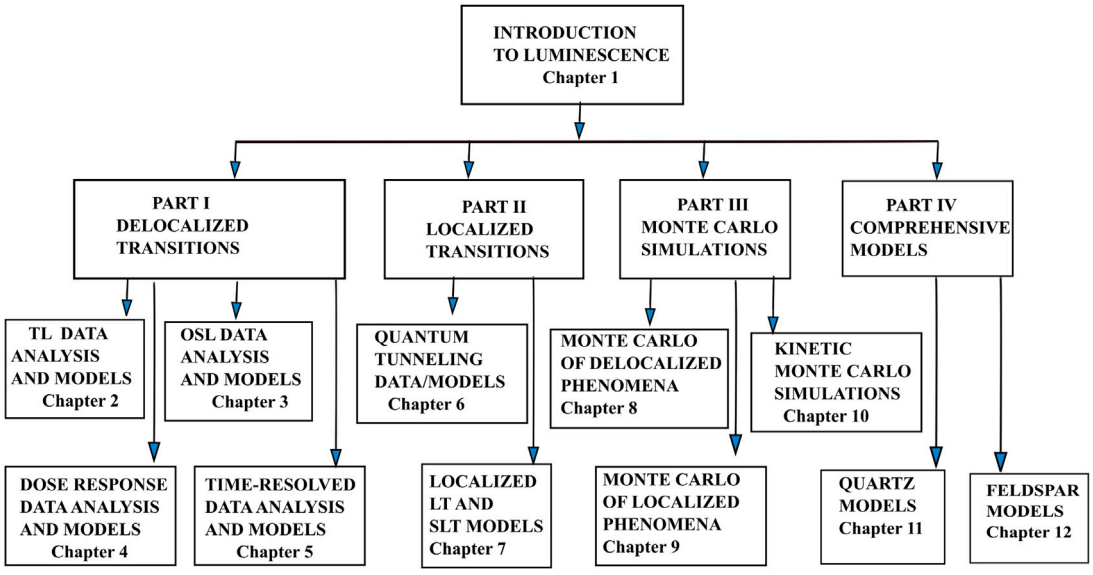

Fig. 7. The organization of the 99 R codes in the recently published book by Pagonis 2021.

7. Conclusions

The purpose of this paper is to describe a new extensive initiative which pools existing models and deconvolution methods for the analysis and modeling of luminescence signals, production transparently, and to develop open-source Python and R software, which can be shared and further developed in the future by the luminescence dosimetry community.

At the current stage of this initiative, 99 R codes and 24 Python codes are available for downloading and using immediately at the two GitHub websites mentioned previously. We anticipate that the initiative will be completed within the next 6 months, and will contain models for TL, OSL, ESR, dose response and TR signals. The classification, organization and standardization of the computerized analysis and modeling in this initiative is straightforward and extensive. Several of the developed codes use the physically meaningful kinetics described by the Lambert W function, instead of the often used empirical general order kinetics (see Table 3).

In addition to containing the computer codes for analyzing experimental data, the R and Python suites of software discussed in this paper contain also codes for modeling studies. Specifically codes are available for the OTOR, TTOR, IMTS, FOK, GOT, GOK and MOK *delocalized* models of luminescence. In addition, codes are provided for several *localized* transition models (LT, SLT, EST, TA-EST) shown in Fig. 7. Examples of such codes are provided for simulating TL signals, OSL signals, TR-OSL signals and the Dose response of dosimetric signals. In addition,

codes are provided in R for modeling stochastic luminescence processes using Monte Carlo techniques, as well as for several commonly used comprehensive phenomenological models for quartz and feldspars.

It is hoped that the proposed classification and organization of the codes will be a useful tool, especially for newcomers to the field of luminescence dosimetry, and for the broad scientific audience involved in luminescence phenomena research: physicists, geologists, archaeologists, solid state physicists, and scientists using radiation in their research.

Declaration of competing interest

The authors declare that they have no known competing financial interests or personal relationships that could have appeared to influence the work reported in this paper.

References

Adamiec, G., Bluszcz, A., Bailey, R., Garcia-Talavera, M., 2006. Finding model parameters: Genetic algorithms and the numerical modelling of quartz luminescence. Radiat. Meas. 41 (7–8), 897–902. http://dx.doi.org/10.1016/j.radmeas.2006.05.005.

Adamiec, G., Garcia-Talavera, M., Bailey, R.M., de La Torre, P.I., 2004. Application of a genetic algorithm to finding parameter values for numerical simulation of quartz luminescence. Geochronometria 23, 9–14.

Afouxenidis, D., Polymeris, G.S., Tsirliganis, N.C., Kitis, G., 2012. Computerised curve deconvolution of TL/OSL curves using a popular spreadsheet program. Radiat. Prot. Dosim. 149, 363–370. http://dx.doi.org/10.1093/rpd/ncr315.

Anechitei-Deacu, V., Timar-Gabor, A., Thomsen, K.J., Buylaert, J.-P., Jain, M., Bailey, M., Murray, A.S., 2018. Single and multi-grain OSL investigations in the high dose range using coarse quartz. Radiat. Meas. 120, 124–130. http://dx.doi.org/10.1016/j.radmeas.2018.06.008.

Balian, H.G., Eddy, N.W., 1977. Figure-of-merit (FOM), an improved criterion over the normalized chi-squared test for assessing goodness-of-fit of gamma-ray spectral peaks. Nucl. Instrum. Methods 145, 389–395. http://dx.doi.org/10.1016/0029-554x(77)90437-2.

Berger, G., 1990. Regression and error analysis for a saturating-exponential-plus-linear model. Ancient TL 8 (3), 23–25.

Berger, G.W., Chen, R., 2011. Error analysis and modelling of double saturating exponential dose response curves from SAR osl dating. Ancient TL 29 (1), 9–14.

Bosken, J.J., Schmidt, C., 2020. Direct and indirect luminescence dating of tephra: A review. J. Quat. Sci. 35 (1–2), 39–53. http://dx.doi.org/10.1002/jqs.3160, URL https://onlinelibrary.wiley.com/doi/abs/10.1002/jqs.3160.

Bowman, S.G.E., Chen, R., 1979. Superlinear filling of traps in crystals due to competition during irradiation. J. Lumin. 18–19, 345–348. http://dx.doi.org/10.1016/0022-2313(79)90136-4.

Chen, R., McKeever, S.W.S., 1997. Theory of Thermoluminescence and Related Phenomena. World Scientific, Singapore.

Chen, R., Pagonis, V., 2011. Thermally and Optically Stimulated Luminescence: A Simulation Approach. John Wiley & Sons, Chichester.

Chithambo, M.L., Ankjærgaard, C., Pagonis, V., 2016. Time-resolved luminescence from quartz: An overview of contemporary developments and applications. Physica B 481, 8–18.

Chung, K., Choe, H., Lee, J., Kim, J., 2011. An algorithm for the deconvolution of the optically stimulated luminescence glow curves involving the mutual interactions among the electron traps. Radiat. Meas. 46 (12), 1598–1601. http://dx.doi.org/10.1016/j.radmeas.2011.05.071.

Chung, K., Lee, J., Kim, J., 2012. A computer program for the deconvolution of the thermoluminescence glow curves by employing the interactive trap model. Radiat. Meas. 47 (9), 766–769. http://dx.doi.org/10.1016/j.radmeas.2012.03.026.

Chung, K., Park, C., Lee, J., Kim, J., 2013. Thermoluminescence glow curve deconvolution of lif:Mg,cu,si with more realistic kinetic models. Radiat. Meas. 59, 151–154. http://dx.doi.org/10.1016/j.radmeas.2013.05.006.

Comprehensive R. Archive Network (CRAN), 2022. CRAN - Package minpack.lm. URL https://cran.r-project.org/web/packages/minpack.lm/index.html.

Corless, R.M., Gonnet, G.H., Hare, D.G.E., Jerey, D.J., Knuth, D.E., 1996. On the Lambert W function. Adv. Comput. Math. 5, 329–359.

Corless, R.M., Jerey, D.J., Knuth, D.E., 1997. A sequence series for the Lambert W function. In: In Proceedings of the International Symposium on Symbolic and Algebraic Computation. ISSAC, pp. 133–140.

Duval, M., 2012. Dose response curve of the ESR signal of the aluminum center in quartz grains extracted from sediment. Ancient TL 30 (2), 1–9.

Fuchs, M., Kreutzer, S., Rousseau, D., Antoine, P., Hatté, C., Lagroix, F., Moine, O., Gauthier, C., Svoboda, J., Lisá, L., 2013. The loess sequence of Dolní Věstonice, Czech Republic: A new OSL-based chronology of the last climatic cycle. Boreas 42 (3), 664–677.

Gómez-Ros, J.M., Kitis, G., 2002. Computerized glow-curve deconvolution using mixed and general order kinetics. Radiat. Prot. Dosim. 101, 47–52.

Jain, M., Guralnik, B., Andersen, M.T., 2012. Stimulated luminescence emission from localized recombination in randomly distributed defects. J. Phys.: Condens. Matter 24 (38), 385402.

Kitis, G., Carinou, E., Askounis, P., 2012. Glow-curve de-convolution analysis of TL glow-curve from constant temperature hot gas TLD readers. Radiat. Meas. 47, 258–265. http://dx.doi.org/10.1016/j.radmeas.2012.02.010, URL http://www.sciencedirect.com/science/article/pii/S1350448712000571.

Kitis, G., Gómez-Ros, J.M., 1999. Glow curve deconvolution functions for mixed order kinetics and a continuous trap distribution. Nucl. Instrum. Methods A 440 440, 224–231.

Kitis, G., Gómez-Ros, J.M., Tuyn, J.W.N., 1998. Thermoluminescence glow curve deconvolution functions for first, second and general order kinetics. J. Phys. D: Appl. Phys. 31, 2646–2666.

Kitis, G., Pagonis, V., 2008. Computerized curve deconvolution analysis for LM-OSL. Radiat. Meas. 43, 737–741.

Kitis, G., Pagonis, V., 2013. Analytical solutions for stimulated luminescence emission from tunneling recombination in random distributions of defects. J. Lumin. 137, 109–115. http://dx.doi.org/10.1016/j.jlumin.2012.12.042.

Kitis, G., Pagonis, V., 2014. Properties of thermoluminescence glow curves from tunneling recombination processes in random distributions of defects. J. Lumin. 153, 118–124. http://dx.doi.org/10.1016/j.jlumin.2014.03.014.

Kitis, G., Polymeris, G.S., Pagonis, V., 2019. Stimulated luminescence emission: From phenomenological models to master analytical equations. Appl. Radiat. Isot. 153, 108797. http://dx.doi.org/10.1016/j.apradiso.2019.05.041.

Kitis, G., Polymeris, G.S., Sfampa, I.K., Prokic, M., Meriç, N., Pagonis, V., 2016. Prompt isothermal decay of thermoluminescence in Mg_4BO_7: Dy, Na and Li_4Bo_7:Cu,in dosimeters. Radiat. Meas. 84, 15–25. http://dx.doi.org/10.1016/j.radmeas.2015.11.002, URL http://www.sciencedirect.com/science/article/pii/S1350448715300731.

Kitis, G., Vlachos, N.D., 2013. General semi-analytical expressions for TL, OSL and other luminescence stimulation modes derived from the OTOR model using the Lambert W-function. Radiat. Meas. 48, 47–54. http://dx.doi.org/10.1016/j.radmeas.2012.09.006.

Kreutzer, S., Burow, C., Dietze, M., Fuchs, M.C., Fischer, M., Schmidt, C., 2017. Software in the context of luminescence dating: status, concepts and suggestions exemplified by the R package luminescence. Ancient TL 35 (2).

Kreutzer, S., Schmidt, C., Fuchs, M.C., Dietze, M., Fischer, M., Fuchs, M., 2012. Introducing an R package for luminescence dating analysis. Ancient TL 30 (1), 1–8.

Li, B., Jacobs, Z., Roberts, R.G., 2016. Investigation of the applicability of standardised growth curves for OSL dating of quartz from Haua Fteah cave, Libya. Quat. Geochronol. 35, 1–15. http://dx.doi.org/10.1016/j.quageo.2016.05.001, URL http://www.sciencedirect.com/science/article/pii/S1871101416300425.

Lowick, S.E., Preusser, F., Wintle, A.G., 2010. Investigating quartz optically stimulated luminescence dose response curves at high doses. Radiat. Meas. 45 (9), 975–984. http://dx.doi.org/10.1016/j.radmeas.2010.07.010.

Mandowski, A., Bos, A.J.J., 2011. Explanation of anomalous heating rate dependence of thermoluminescence in YPO_4:Ce^{3+},Sm^{3+} based on the semilocalized transition (SLT) model. Radiat. Meas. 46, 1376–1379. http://dx.doi.org/10.1016/j.radmeas.2011.05.018, URL http://www.sciencedirect.com/science/article/pii/S1350448711001855.

Moré, J.J., 1977. The levenberg-marquardt algo-rithm: Implementation and theory.

Pagonis, V., 2021. Luminescence: Data Analysis and Modeling using R. In: Use R!, Springer International Publishing, URL https://www.springer.com/us/book/9783030673109.

Pagonis, V., Ankjærgaard, C., Jain, M., Chithambo, M.L., 2016. Quantitative analysis of time-resolved infrared stimulated luminescence in feldspars. Physica B 497, 78–85.

Pagonis, V., Brown, N.D., Peng, J., Kitis, G., Polymeris, G.S., 2021. On the deconvolution of promptly measured luminescence signals in feldspars. J. Lumin. 239, 118334. http://dx.doi.org/10.1016/j.jlumin.2021.118334.

Pagonis, V., Brown, N., Polymeris, G.S., Kitis, G., 2019. Comprehensive analysis of thermoluminescence signals in Mg_4Bo_7: Dy, Na dosimeter. J. Lumin. 213, 334–342. http://dx.doi.org/10.1016/j.jlumin.2019.05.044.

Pagonis, V., Kitis, G., 2015. Mathematical aspects of ground state tunneling models in luminescence materials. J. Lumin. 168, 137–144.

Pagonis, V., Kitis, G., Chen, R., 2020a. A new analytical equation for the dose response of dosimetric materials, based on the Lambert W function. J. Lumin. 225, 117333. http://dx.doi.org/10.1016/j.jlumin.2020.117333.

Pagonis, V., Kitis, G., Chen, R., 2020b. Superlinearity revisited: A new analytical equation for the dose response of defects in solids, using the Lambert W function. J. Lumin. 227, 117553. http://dx.doi.org/10.1016/j.jlumin.2020.117553.

Pagonis, V., Mian, S.M., Kitis, G., 2001. Fit of first order thermoluminescence glow peaks using the Weibull distribution function. Radiat. Prot. Dosim. 93, 11–17. http://dx.doi.org/10.1093/oxfordjournals.rpd.a006406.

Pagonis, V., Morthekai, P., Singhvi, A.K., Thomas, J., Balaram, V., Kitis, G., Chen, R., 2012. Time-resolved infrared stimulated luminescence signals in feldspars: Analysis based on exponential and stretched exponential functions. J. Lumin. 132 (9), 2330–2340.

Peng, J., Dong, Z., Han, F., 2016. Tgcd: An R package for analyzing thermoluminescence glow curves. SoftwareX 5, 112–120. http://dx.doi.org/10.1016/j.softx.2016.06.001.

Peng, J., Kitis, G., Sadek, A.M., Karsu Asal, E.C., Li, Z., 2021. Thermoluminescence glow-curve deconvolution using analytical expressions: A unified presentation. Appl. Radiat. Isot. 168, 109440. http://dx.doi.org/10.1016/j.apradiso.2020.109440.

Polymeris, G.S., Pagonis, V., Kitis, G., 2017. Thermoluminescence glow curves in preheated feldspar samples: An interpretation based on random defect distributions. Radiat. Meas. 97, 20–27. http://dx.doi.org/10.1016/j.radmeas.2016.12.012.

Polymeris, G.S., Sfampa, I.K., Niora, M., Malletzidou, E.C.S.L., Giannoulatou, V., Pagonis, V., Kitis, G., 2018. Anomalous fading in TL, OSL and TA OSL signals of durango apatite for various grain size fractions; from micro to nano scale. J. Lumin. 195, 216–224.

Puchalska, M., Bilski, P., 2006. GlowFit-a new tool for thermoluminescence glow-curve deconvolution. Radiat. Meas. 41 (6), 659–664. http://dx.doi.org/10.1016/j.radmeas.2006.03.008.

Sadek, A.M., Eissa, H.M., Basha, A.M., Carinou, E., Askounis, P., Kitis, G., 2015. The deconvolution of thermoluminescence glow-curves using general expressions derived from the one trap-one recombination (OTOR) level model. Appl. Radiat. Isot.: Includ. Data Instrum. Methods Agric. Ind. Med. 95, 214–221. http://dx.doi.org/10.1016/j.apradiso.2014.10.030.

Şahiner, E., Kitis, G., Pagonis, V., Meriç, N., Polymeris, G.S., 2017. Tunnelling recombination in conventional, post-infrared and post-infrared multi-elevated temperature IRSL signals in microcline K-feldspar. J. Lumin. 188, 514–523.

Sfampa, I.K., Polymeris, G.S., Pagonis, V., Theodosoglou, E., Tsirliganis, N., Kitis, G., 2015. Correlation of basic TL, OSL and IRSL properties of ten K-feldspar samples of various origins. Nucl. Instrum. Methods Phys. Res. B 359, 89–98. http://dx.doi.org/10.1016/j.nimb.2015.07.106, URL http://www.sciencedirect.com/science/article/pii/S0168583X15006849.

Sfampa, I.K., Polymeris, G.S., Tsirliganis, N., Pagonis, V., Kitis, G., 2014. Prompt isothermal decay of thermoluminescence in an apatite exhibiting strong anomalous fading. Nucl. Instrum. Methods Phys. Res. B 320, 57–63. http://dx.doi.org/10.1016/j.nimb.2013.12.003, URL http://www.sciencedirect.com/science/article/pii/S0168583X13011646.

Singh, L.L., Gartia, R.K., 2013. Theoretical derivation of a simplified form of the OTOR/GOT differential equation. Radiat. Meas. 59, 160–164. http://dx.doi.org/10.1016/j.radmeas.2013.04.022, URL http://www.sciencedirect.com/science/article/pii/S1350448713002163.

Timar-Gabor, A., Constantin, D., Buylaert, J.P., Jain, M., Murray, A.S., Wintle, A.G., 2015. Fundamental investigations of natural and laboratory generated SAR dose response curves for quartz OSL in the high dose range. Radiat. Meas. 81, 150–156. http://dx.doi.org/10.1016/j.radmeas.2015.01.013, URL http://www.sciencedirect.com/science/article/pii/S1350448715000141.

Timar-Gabor, A., Vasiliniuc, A., Vandenberghe, D.A.G., Cosma, C., Wintle, A.G., 2012. Investigations into the reliability of SAR-osl equivalent doses obtained for quartz samples displaying dose response curves with more than one component. Radiat. Meas. 47 (9), 740–745. http://dx.doi.org/10.1016/j.radmeas.2011.12.001, URL http://www.sciencedirect.com/science/article/pii/S1350448711005671.

Trompier, F., Bassinet, C., Della Monaca, S., Romanyukha, A., Reyes, R., Clairand, I., 2011. Overview of physical and biophysical techniques for accident dosimetry. Radiat. Prot. Dosim. 144, 571–574. http://dx.doi.org/10.1093/rpd/ncq341.

Van Rossum, G., Drake, F.L., 2009. Python 3 Reference Manual. CreateSpace, Scotts Valley, CA.

Vandenberghe, D.A.G., Jain, M., Murray, A.S., 2009. Equivalent dose determination using a quartz isothermal TL signal. Radiat. Meas. 44 (5), 439–444. http://dx.doi.org/10.1016/j.radmeas.2009.03.006.